第 36 卷第 6 期
2020 年 6 月

无 机 化 学 学 报
CHINESE JOURNAL OF INORGANIC CHEMISTRY

Vol.36 No.6
1131-1136

一例可分离的双核铁氢自由基阳离子

唐树轩[1] 张 莉[2] 阮华棚[1] 赵 越[1] 谭庚文*,[1,3] 王新平*,[1]

([1]南京大学化学化工学院,配位化学国家重点实验室,江苏省先进有机材料重点实验室,人工微结构科学与技术协同创新中心,南京 210023)

([2]广西科技大学材料科学与工程中心,柳州 545006)

([3]苏州大学材料与化学化工学部,苏州 215123)

摘要：成功分离得到了一例双核铁氢自由基阳离子盐 *cis*-$[Fe_2Cp_2(\mu\text{-}H)(\mu\text{-}PPh_2)(CO)_2]^{\cdot+}[Al(OC(CF_3)_3)_4]^-$(*cis*-**1**$^{\cdot+}$$[Al(OC(CF_3)_3)_4]^-$)晶体，并使用单晶 X 射线衍射、电子顺磁共振、红外光谱、紫外–可见光谱以及密度泛函理论对它进行了表征和理论计算。电子顺磁共振和密度泛函理论计算分析表明，自由基的自旋密度主要均等分布于 2 个铁原子上。

关键词：过渡金属氢化物；自由基阳离子；铁氢自由基阳离子；弱配位阴离子

中图分类号：O614.81$^+$1；O614.3$^+$1　　**文献标识码**：A　　**文章编号**：1001-4861(2020)06-1131-06

DOI：10.11862/CJIC.2020.115

An Isolable Dinuclear Iron Hydride Radical Cation

TANG Shu-Xuan[1] ZHANG Li[2] RUAN Hua-Peng[1]

ZHAO Yue[1] TAN Geng-Wen*,[1,3] WANG Xin-Ping*,[1]

([1]*State Key Laboratory of Coordination Chemistry, Jiangsu Key Laboratory of Advanced Organic Materials, School of Chemistry and Chemical Engineering, Collaborative Innovation Center of Advanced Microstructures, Nanjing University, Nanjing* 210023, *China*)

([2]*Center of Materials Science and Engineering, Guangxi University of Science and Technology, Liuzhou, Guangxi* 545006, *China*)

([3]*College of Chemistry, Chemical Engineering and Materials Science, Soochow University, Suzhou, Jiangsu* 215123, *China*)

Abstract: The dinuclear iron hydride radical cation salt *cis*-$[Fe_2Cp_2(\mu\text{-}H)(\mu\text{-}PPh_2)(CO)_2]^{\cdot+}[Al(OC(CF_3)_3)_4]^-$ (*cis*-**1**$^{\cdot+}$$[Al(OC(CF_3)_3)_4]^-$) was isolated as a crystalline solid. It has been characterized by single crystal X-ray crystallography, electron paramagnetic resonance (EPR), infrared, and UV-Vis spectroscopy, in conjunction with density functional theory (DFT) calculations. EPR and DFT calculation studies reveal that the spin density of the radical is mainly equally located at both of the iron atoms. CCDC: 1910053.

Keywords: transition metal hydride; radical cations; iron hydride radical cations; weakly coordinating anion

0 Introduction

Transition metal hydride radical cations (TMHRCs) have been the research focus for a long time because of their pivotal roles in various organic reactions and biological processes[1], such as proton-coupled electron transfer[2], hydrogen activation[3], and catalytic hydrogenation reactions[4]. In contrast to the closed-shell transition metal hydrides, TMHRCs have an open shell electronic configuration, thus they are

收稿日期：2020-02-10。收修改稿日期：2020-03-13。

国家重点研究发展计划(No.2016YFA0300404，2018YFA0306004)，国家自然科学基金(No.21525102，21690062，21601082)和中央高校基本科研专项资金(No.14380191，14380194)资助项目。

*通信联系人。E-mail：gwtan@suda.edu.cn，xpwang@nju.edu.cn

generally highly reactive and the stabilization of TMHRCs is quite challenging due to the presence of fragile TM-hydride bonds, which easily undergo homolytical or heterolytical cleavage[1a]. Until now, numbers of TMHRCs have been observed and characterized in solution phase[5], such as niobium hydride[6], molybdenum hydride[7], tungsten hydride[8], ruthenium hydride[9] and copper hydride[10]. However, there are few stable first-row TMHRCs having been isolated and structurally characterized[11-12].

The iron hydride species have been discovered and investigated as key intermediates in catalysis[13], biological processes[14], energy storage and transfer[15]. Although lots of efforts have been devoted to the synthesis and characterization of new iron hydride radical cations, most of them only exist in solution phase and are only stable under low temperature, making them difficult to be isolated in solid state[16]. For example, the dinuclear iron hydride radical cation *cis*-$[Fe_2Cp_2(\mu\text{-}H)(\mu\text{-}PPh_2)(CO)_2]^{\cdot+}$ was synthesized and characterized by electron paramagnetic resonance (EPR) and infrared spectroscopy (IR) in the solution phase in 2004[16b]. However, this radical cation was quite air-sensitive and decomposed easily at room tempera μture, which hindered the further research. Until now, there are only few examples of iron hydride radical cations that have been isolated[12], including $[Fe(Cp^*)(dppe)H]^{\cdot+}$ (dppe=l,2-bis(diphenyl phosphino)ethane, $Cp^*=\eta\text{-}C_6Me_5$) radical cation[12a-12b], $[Fe(Cp^*)(dcpe)H]^{\cdot+}$ ($dcpe=1,2\text{-}C_2H_4(PCy_2)_2$;) radical cation[12c], and $[Cp^*Fe(pdt)Fe(dppe)(CO)H]^{\cdot+}$ ($pdt^{2-}=CH_2(CH_2S^-)_2$) radical cation[12d].

By the aid of weakly coordinating anions, we have recently successfully obtained several main-group element- and transition metal-centred radical cations[17]. Inspired by these previous work, we were interested in stabilizing iron hydride radical cations by employing the weakly coordinating anion $[Al(OC(CF_3)_3)_4]^-$ [18]. Herein, we report the synthesis and characterization of the isolable dinuclear iron hydride radical cation salt *cis*-$[Fe_2Cp_2(\mu\text{-}H)(\mu\text{-}PPh_2)(CO)_2]^{\cdot+}[Al(OC(CF_3)_3)_4]^-$ (*cis*-$\mathbf{1}^{\cdot+}[Al(OC(CF_3)_3)_4]^-$), in which the spin density mainly resides at the iron centers.

1 Experimental

1.1 Materials and methods

All experiments were carried out under a nitrogen atmosphere by using standard Schlenk techniques and an argon-filled glovebox. Solvents were purified under standard procedures. *Trans*-**1**[16b] and $Ag[Al(OC(CF_3)_3)_4]$[18] were synthesized according to the literature methods. Single crystal X-ray diffraction was carried out by using a Bruker D8 CMOS detector at 173 K. The structures were solved by direct methods and all refined on F^2 with the SHELX-2018 software package [19]. The H atom of the Fe-H-Fe moiety in *cis*-$\mathbf{1}^{\cdot+}$ was positioned from difference Fourier maps and refined freely. Infrared spectra were collected on VECTOR22 FT-IR spectrometer, using KBr pellet. EPR spectra were obtained using a Bruker EMX plus-6/1 variable-temperature apparatus, and were simulated using WINEPR SimFonia. UV-Vis spectra were recorded on the Lambda 750 spectrometer. Element analyses were performed at Shanghai Institute of Organic Chemistry, the Chinese Academy of Sciences.

CCDC: 1910053.

1.2 Synthesis of *cis*-$\mathbf{1}^{\cdot+}[Al(OC(CF_3)_3)_4]^-$

Trans-**1** (97 mg, 0.2 mmol) and $Ag[Al(OC(CF_3)_3)_4]$ (215 mg, 0.2 mmol) were added into a 100 mL Schlenk flask. The temperature was cooled down to 233 K and chlorobenzene (50 mL) was added via cannula. The mixture was warmed up to r.t. naturally and stirred overnight. Then the brown mixture was filtered and the filtrate was concentrated. The reddish brown crystal of *cis*-$\mathbf{1}^{\cdot+}[Al(OC(CF_3)_3)_4]^-$ was obtained by leaving the concentrated solution at 263 K for one week. The crude product was purified by recrystallization from a hexane/chlorobenzene mixed solution at 263 K. Yield: 0.13 g, 48%; Element analysis Calcd. for $C_{40}H_{21}AlF_{36}Fe_2O_6P$(%): C 33.11, H 1.46; Found(%): C 32.81, H 1.55.

2 Results and discussion

The radical cation salt *cis*-$\mathbf{1}^{\cdot+}[Al(OC(CF_3)_3)_4]^-$ was synthesized by selective one-electron oxidation of *trans*-**1**[16b] with $Ag[Al(OC(CF_3)_3)_4]$[18] in chlorobenzene at room temperature (Fig.1a). It is highly sensitive to

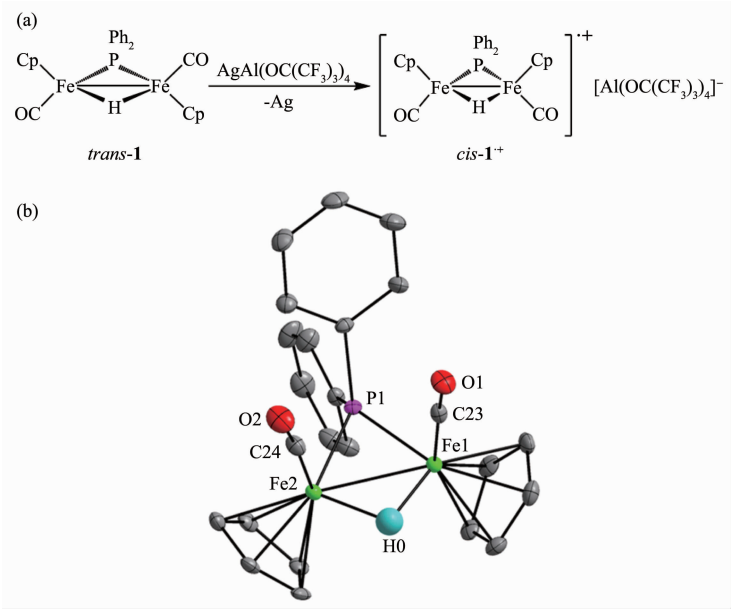

All hydrogen atoms except the hydride are not shown for clarity in (b); Selected bond lengths (nm) and angles (°): Fe1-Fe2 0.257 00(9), Fe1-P1 0.219 65(13), Fe2-P1 0.219 78(11), Fe1-H0 0.163 34, Fe2-H0 0.172 07, O2-C24-Fe2 174.3(4), O1-C23-Fe1 177.3(4), Fe1-Fe2-H0 38.700, Fe2-Fe1-H0 41.200, Fe1-Fe2-P1 54.18(4), Fe2-Fe1-P1 54.23(3), H0-Fe1-C23 97.900, P1-Fe1-C23 90.61(2), H0-Fe2-C24 101.60, P1-Fe2-C24 92.17(1)

Fig.1　(a) Synthesis of *cis*-**1**$^{\cdot+}$[Al(OC(CF$_3$)$_3$)$_4$]$^-$; (b) Thermal ellipsoid (30%) drawing of *cis*-**1**$^{\cdot+}$

oxygen and moisture, but can be stored in an N_2 atmosphere for months. It has been fully characterized by single crystal X-ray diffraction, EPR, IR and UV-Vis spectroscopy, in conjunction with theoretical calculations.

The crystal structure of *cis*-**1**$^{\cdot+}$, including the selected bond distances and angles, are shown in Fig. 1b. The salient feature is the *cis* configuration of the two cyclopentadienyl (Cp) groups in *cis*-**1**$^{\cdot+}$, in contrast to the *trans* form in the starting material *trans*-**1** [20]. This is consistent with the observation of fast isomerization of *trans*-**1**$^{\cdot+}$ to *cis*-**1**$^{\cdot+}$ in solution[16b]. The Fe-Fe bond distance decreases from 0.270 98(3) to 0.257 00(9) nm, and the Fe-P bond distances increase from 0.218 36(4), 0.219 40(4) nm to 0.219 65(13), 0.219 78(11) nm upon one-electron oxidation. This indicates that the interaction between the iron atoms becomes stronger, while the interaction between the iron atom and the phosphorus atom becomes weaker. Although the conformation has changed, bond cleavage does not happen. The two iron atoms are still connected by the diphenylphosphide ligand and the bridging hydrogen atom, and each iron atom remains coordinating with one carbonyl ligand and one Cp ligand.

In the IR spectrum of *cis*-**1**$^{\cdot+}$[Al(OC(CF$_3$)$_3$)$_4$]$^-$, the absorption peaks of the carbonyl groups were at 1 990 and 2 029 cm^{-1}, which were blue-shifted in comparison to those of the neutral compound *trans*-**1** (1 855 and 1 898 cm^{-1}) (Fig.2). According to Dewar-Chatt-Duncanson model, it can be interpreted by the decreasing of backdonation from the Fe centers to the carbonyl groups due to the removal of one electron.

The EPR spectra of *cis*-**1**$^{\cdot+}$[Al(OC(CF$_3$)$_3$)$_4$]$^-$ were recorded at 298 K in solution and solid state, and the results were simulated by WinEPR SimFonia (Fig.3).

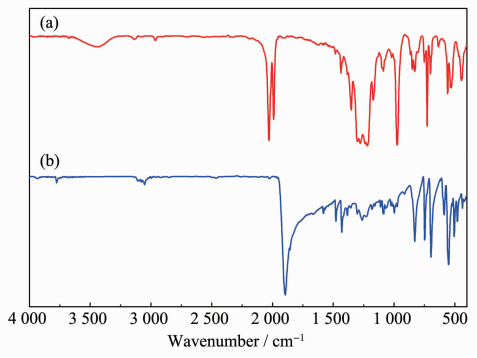

Fig.2　IR spectra of (a) *cis*-**1**$^{\cdot+}$[Al(OC(CF$_3$)$_3$)$_4$]$^-$ and (b) *trans*-**1**

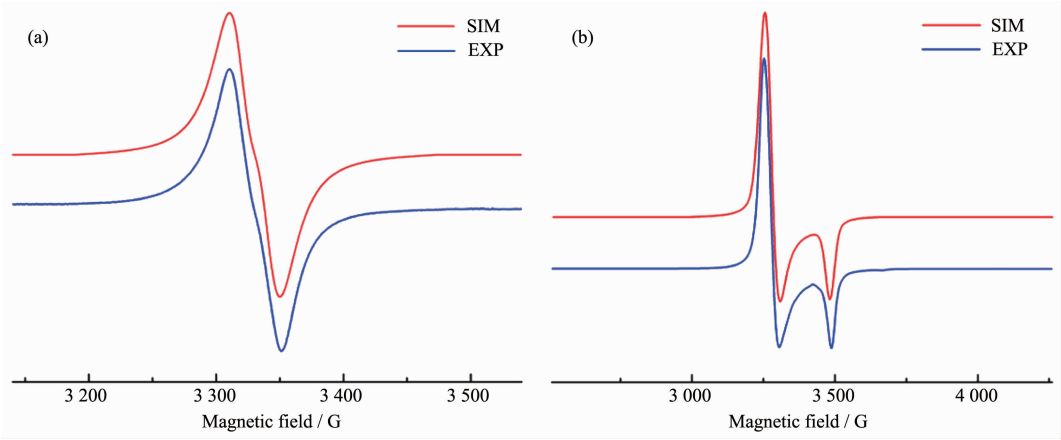

Fig.3 (a) Solution EPR spectrum of 1 μmol·L^{-1} *cis*-**1**$^{\cdot+}$[Al(OC(CF$_3$)$_3$)$_4$]$^-$ in chlorobenzene at 298 K; (b) Powder EPR spectrum of *cis*-**1**$^{\cdot+}$[Al(OC(CF$_3$)$_3$)$_4$]$^-$ at 298 K

The solution EPR spectrum exhibited a relatively broad isotropic signal at g=2.113, which deviated from the g value of free electron (g=2.002 3), but was close to the iron-centred radical [FeH(dppe)$_2$] (g=2.085)[16d], suggesting the free electron has a strong interaction with the iron nuclei. The coupling with one phosphorus nucleus (a(^{31}P)=20 G) was included to get a best simulation result. The room temperature powder spectrum displayed an anisotropic spectrum with g_x= 2.156, g_y=2.128, and g_z=2.023, which were also close to the g factors of the paramagnetic iron hydride complex [FeHCl(dppe)$_2$][ClO$_4$] (g_x=2.185, g_y=2.100, and g_z=1.981)[16d].

Density functional theory (DFT) calculations[21] have been used to get more insight into the electronic structure of *cis*-**1**$^{\cdot+}$ (Fig.4). The crystal structure was well reproduced by calculation at the UB3LYP/ LanL2DZ/6-31G(d) level of theory (Table 1, S2 and S3). The calculation results revealed that the Wiberg bond order of the Fe-Fe bond increases from 0.464 9 to 0.659 8, while the Wiberg bond orders of the Fe-P bond decrease from 0.919 3, 0.919 1 to 0.894 8, 0.894 6 upon one-electron oxidation. The result is consistent with the changes of bond distances observed in single crystal X-ray diffraction. In addition, the bond orders of the Fe-Fe and Fe-H bonds were close to 0.5 in both *trans*-**1** and *cis*-**1**$^{\cdot+}$, which indicate that there

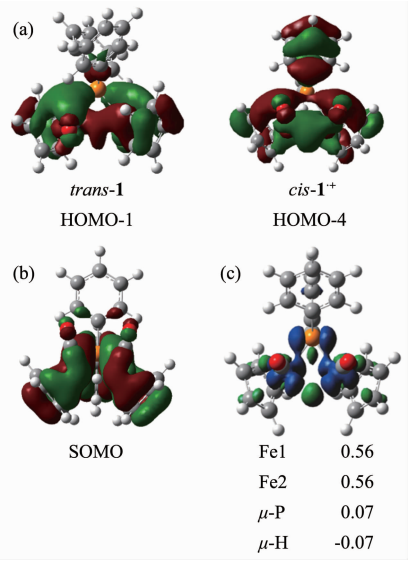

Isovalue: 0.02 in (a) and (b); 0.002 in (c)

Fig.4 (a) Three-center two-electron bond in *trans*-**1** and *cis*-**1**$^{\cdot+}$; (b) SOMO; (c) Spin density of *cis*-**1**$^{\cdot+}$

Table 1 Bond distances and DFT calculated Wiberg bond order of *trans*-1 and *cis*-1$^{\cdot+}$

	trans-**1** bond distance/nm	*trans*-**1** bond order	*cis*-**1**$^{\cdot+}$ bond distance/nm	*cis*-**1**$^{\cdot+}$ bond order
Fe1-Fe2	0.270 98(3)	0.464 9	0.257 00(9)	0.659 8
Fe1-P1	0.218 36(4)	0.919 3	0.219 65(13)	0.894 8
Fe2-P1	0.219 40(4)	0.919 1	0.219 78(11)	0.894 6
Fe1-H0	0.162(2)	0.411 5	0.163 34	0.415 4
Fe2-H0	0.166(2)	0.411 7	0.172 07	0.415 1

should be a three-center two-electron (3-c-2) bond present among the hydrogen atom and two iron atoms. The 3-c-2 bond was represented by the HOMO-1 in *trans*-**1**, and HOMO-4 in *cis*-**1**$^{\cdot+}$ (Fig.4a). The singly occupied molecular orbital (SOMO) as well as the spin density are mainly distributed among the Fe fragments, which indicates that the free electron is mainly located on each iron atom (Fig.4b and 4c).

The UV-Vis absorption spectra of *trans*-**1** and *cis*-**1**$^{\cdot+}$[Al(OC(CF$_3$)$_3$)$_4$]$^-$ were recorded in chlorobenzene solution at room temperature (Fig.5). The spectrum of *trans*-**1** revealed three absorption peaks at 436, 503, and 700 nm, while the spectrum of *cis*-**1**$^{\cdot+}$[Al(OC(CF$_3$)$_3$)$_4$]$^-$ showed four peaks maxima at 445, 591, 688, and 1 200 nm. Judging from the time-dependent DFT (TD-DFT) calculations at UB3LYP/LanL2DZ/6-31G (d) level of theory, the absorptions of *cis*-**1**$^{\cdot+}$[Al(OC(CF$_3$)$_3$)$_4$] at 591, 688, and 1 200 nm are mainly assigned to SOMO→LUMO (α), HOMO-4 (β)→LUMO (β), and HOMO-1(β)→LUMO (β) electronic transitions, respectively (Table S5 in Supporting information).

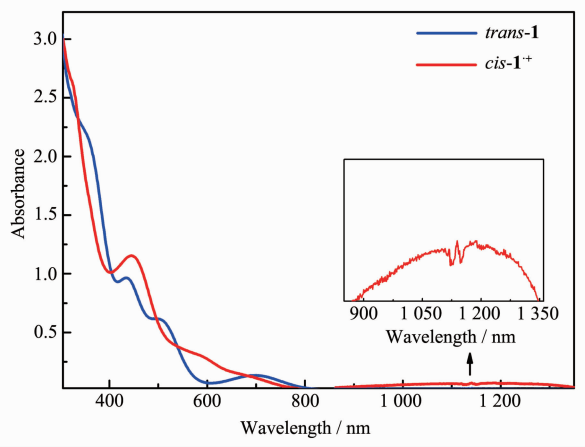

Fig.5 Absorption spectra of 0.1 mmol·L^{-1} *trans*-**1** and *cis*-**1**$^{\cdot+}$[Al(OC(CF$_3$)$_3$)$_4$]$^-$ in chlorobenzene at 298 K

3 Conclusions

In summary, we have successfully isolated and fully characterized the stable dinuclear iron hydride radical cation *cis*-**1**$^{\cdot+}$, in which the Cp ligands feature a *cis* conformation, in contrast to the *trans* form in the precursor *trans*-**1**. The EPR and theoretical calculations reveal that the spin density mainly resides at the iron centers. The synthesis of other TMHRCs and their reactivity studies are currently going on in our laboratory.

Supporting information is available at http://www.wjhxxb.cn

Acknowledgments: We thank the National Key R&D Program of China (Grants No. 2016YFA0300404, 2018YFA0306004, X.W.), the National Natural Science Foundation of China (Grants No. 21525102, 21690062, X.W., 21601082, G.T.), and the Fundamental Research Funds for the Central Universities (Grants No. 14380191, X.W., 14380194, G. T.) for financial support. The calculations were performed at the High-Performance Computing Center of Nanjing University.

References:

[1] (a)Hu Y, Shaw A P, Estes D P, et al. *Chem. Rev.*, **2016**,**116**:8427-8462
(b)Wiedner E S, Chambers M B, Pitman C L, et al. *Chem. Rev.*, **2016**,**116**:8655-8692
(c)Schilter D, Camara J M, Huynh M T, et al. *Chem. Rev.*, **2016**,**116**:8693-8749

[2] (a)Liu T F, Guo M Y, Orthaber A, et al. *Nat. Chem.*, **2018**, **10**:881-887
(b)Huang T, Rountree E S, Traywick A P, et al. *J. Am. Chem. Soc.*, **2018**,**140**:14655-14669
(c)Bourrez M, Steinmetz R, Ott S, et al. *Nat. Chem.*, **2014**,**7**:140-145

[3] (a)Ogata H, Lubitz W, Higuchi Y. *Dalton Trans.*, **2009**:7577-7587
(b)Frey M. *ChemBioChem*, **2002**,**3**:153-160
(c)Evans D J, Pickett C J. *Chem. Soc. Rev.*, **2003**,**32**:268-275
(d)Lubitz W, Ogata H, Rüdiger O, et al. *Chem. Rev.*, **2014**, **114**:4081-4148
(e)Hembre R T, Scott McQueen J, Day V W. *J. Am. Chem. Soc.*, **1996**,**118**:798-803

[4] Shaw A P, Ryland B L, Franklin M J, et al. *J. Org. Chem.*, **2008**,**73**:9668-9674

[5] (a)Ryan O B, Tilset M, Parker V D. *J. Am. Chem. Soc.*, **1990**, **112**:2618-2626
(b)Roberts J A S, Appel A M, DuBois D L, et al. *J. Am. Chem. Soc.*, **2011**,**133**:14604-14613

[6] (a)Blaine C A, Ellis J E, Mann K R. *Inorg. Chem.*, **1995**,**34**:1552-1561
(b)Roullier L, Lucas D, Mugnier Y, et al. *J. Organomet. Chem.*, **1990**,**396**:C12-C16

[7] Baya M, Houghton J, Daran J C, et al. *Chem. Eur. J.*, **2007**,

13:5347-5359

[8] Klingler R J, Huffman J C, Kochi J K. *J. Am. Chem. Soc.*, **1980**,**102**:208-216

[9] Ryan O B, Tilset M. *J. Am. Chem. Soc.*, **1991**,**113**:9554-9561

[10]Eberhart M S, Norton J R, Zuzek A, et al. *J. Am. Chem. Soc.*, **2013**,**135**:17262-17265

[11]Bianchini C, Masi D, Mealli C, et al. *Gazz. Chim. Ital.*, **1986**, **116**:201-206

[12](a)Hamor P, Toupet L, Hamon J R, et al. *Organometallics*, **1992**,**11**:1429-1431

(b)Tilset M, Fjeldahl I, Hamon J R, et al. *J. Am. Chem. Soc.*, **2001**,**123**:9984-10000

(c)Zhang F J, Jia J, Dong S L, et al. *Organometallics*, **2016**, **35**:1151-1159

(d)Yu X, Tung C H, Wang W G, et al. *Organometallics*, **2017**, **36**:2245-2253

[13]Nakazawa H, Itazaki M. *Iron Catalysis*: *Fundamentals and Applications*. Plietker B, Ed., Berlin, Heidelberg: Springer-Verlag, **2011**:27-81

[14](a)Volbeda A, Charon M H, Piras C, et al. *Nature*, **1995**, **373**:580-587

(b)Fontecilla-Camps J C, Volbeda A, Cavazza C, et al. *Chem. Rev.*, **2007**,**107**:4273-4303

[15]Liu Y C, Chu K T, Huang Y L, et al. *ACS Catal.*, **2016**,**6**: 2559-2576

[16](a)Bianchini C, Laschi F, Peruzzini M, et al. *Inorg. Chem.*, **1990**,**29**:3394-3402

(b)Alvarez C M, Esther García M, Ruiz M A, et al. *Organometallics*, **2004**,**23**:4750-4758

(c)Jiménez-Tenorio M, Carmen Puerta M, Valerga P. *Organometallics*, **1994**,**13**:3330-3337

(d)Gargano M, Giannoccaro P, Rossi M, et al. *J. Chem. Soc. Dalton Trans.*, **1975**:9-12

[17](a)Zheng X, Wang X Y, Zhang Z C, et al. *Angew. Chem. Int. Ed.*, **2015**,**54**:9084-9087

(b)Wang W Q, Wang X Y, Zhang Z C, et al. *Chem. Commun.*, **2015**,**51**:8410-8413

(c)Li S Y, Wang X Y, Zhang Z C, et al. *Dalton Trans.*, **2015**, **44**:19754-19757

(d)Zheng X, Zhang Z C, Tan G W, et al. *Inorg. Chem.*, **2016**,**55**:1008-1010

(e)Wang W Q, Li J, Yin L, et al. *J. Am. Chem. Soc.*, **2017**, **139**:12069-12075

(f)Tan G W, Wang X P. *Chin. J. Chem.*, **2018**,**36**:573-586

[18]Krossing I. *Chem. Eur. J.*, **2001**,**7**:490-502

[19]Sheldrick G M. *SHELX*-2018, *Program for Crystal Structure Refinement*, University of Göttingen, Germany, **2018**.

[20]Decken A, Craig C D, Bottomley F. *Acta Crystallogr. Sect. E*, **2004**,**E60**:m1284-m1285

[21]Frisch M J, Trucks G W, Schlegel H B, et al. *Gaussian* 09, *Revision B*.01, Gaussian, Inc., Wallingford CT, **2010**.